CHEMISTRY
A EUROPEAN JOURNAL

DOI: 10.1002/chem.200601559

Electrostatic Attachment of Gold and Poly(lactic acid) Nanoparticles onto ω-Aminoalkanoic Acid Self-Assembled Monolayers on 316L Stainless Steel

Galit Shustak,[a, b] Yulia Shaulov,[b] Abraham J. Domb,[b] and Daniel Mandler*[a]

Abstract: The assembly of poly(lactic acid) (PLA) nanoparticles on a 12-aminodecanoic acid (ADA) self-assembled monolayer (SAM) is described. Assembly is accomplished through electrostatic interactions between the positively charged SAM and the negatively charged PLA nanoparticles. The strategy used involves two steps in which a preliminary electrochemical coating of the ADA SAM is followed by a second step that involves immersing the SAM in a solution containing gold or PLA nanoparticles. The SAM was characterized by using cyclic voltammetry (CV), X-ray photoelectron spectroscopy (XPS), FTIR spectroscopy, and contact angle measurements, whereas scanning electron microscopy (SEM) was used to image the nanoparticles after electrostatic attachment was achieved. We found that the surface coverage of the nanoparticles could be controlled by modulating the electrostatic interactions between the negatively charged particles and the positively charged SAM surface by varying the pH of the nanoparticle solution, the immersion time, and the number of cyclic voltammetry scans under which the SAM was formed.

Keywords: electrostatic interactions · monolayers · nanoparticles · polymers · stainless steel

Introduction

Stainless steel is widely used to manufacture implantable medical devices owing to its corrosion resistance and mechanical properties. However, whereas the bulk properties are desirable, the metal surface provokes protein adsorption, platelet adhesion, and complement activation, which leads to the failure of the implanted metal device. Motivated by a need to improve the biocompatibility of the stainless steel surface, researchers have recently focused their efforts on modifying the surface by using biomaterials.[1,2] As a result, a wide range of implantable applications, which include orthopedic, endovascular, and dental devices, in addition to drug delivery systems, have been developed based on biocompatible coatings, such as polymeric thin films and microspheres that contain drugs. Active agents, that is, drugs, have been incorporated into those biocompatible coatings, which results in the formation of drug-eluting implants. One of the advantages of drug-eluting coatings is the fact that drug release is localized, which results in higher tissue drug levels at the specific treated site and decreases the systemic drug-associated side effects.[3–7]

Several approaches have been described for embedding drugs inside thin films.[8] Decher and co-workers developed the layer-by-layer (LBL) deposition technique in which the alternate deposition of polyanions and polycations onto a charged solid substrate led to the formation of multilayers.[9–11] Drugs and other biomaterials can be integrated into these films through covalent bonding or supramolecular interactions.[12–13] In the context of controlled release of a drug, the LBL fabrication procedure offers the ability to control the number and location of the relevant polymer layers. Hence, drug release would be dependent on the permeability or breakdown of the multilayer structure.

Recently we reported electrochemically induced polymer coatings on 316L stainless steel surfaces.[14–17] The aim of those studies was primarily to demonstrate that electropolymerization of conducting polymers was suitable for coating medical devices with a protective layer that improved their surface biocompatibility and allowed controlled release of bioactive agents. Moreover, we showed that the formation of an intermediate organic monolayer prior to electropolymerization significantly promoted adhesion of the polymer

[a] G. Shustak, Prof. D. Mandler
Department of Inorganic and Analytical chemistry
The Hebrew University of Jerusalem
Jerusalem 91904 (Israel)
Fax: (+972) 2-658-5319
E-mail: mandler@vms.huji.ac.il

[b] G. Shustak, Y. Shaulov, Prof. A. J. Domb
Department of Medicinal Chemistry and Natural Products
School of Pharmacy-Faculty of Medicine
The Hebrew University of Jerusalem
Jerusalem 91120 (Israel)

to the surface.[16] However, the amount of drug impregnated into these conducting thin polymers was limited by the swelling capability of the polymeric matrix. The latter can be significantly improved by assembling drug-containing polymeric nanoparticles. Although nanoparticles can be formulated from a wide variety of synthetic and natural polymers, evidently such nanoparticles must be biocompatible and preferably also biodegradable for sustained drug delivery applications.[7] Poly(lactic acid) (PLA) and poly(ethylene glycol) (PEG) have been the most frequently used nanoparticle polymers for sustained and localized administration of different therapeutic agents.[3–6]

A number of strategies have been explored for assembling nanoparticles onto metal surfaces. These strategies include exploiting covalent[18–22] and electrostatic interactions,[32–34] the formation of Langmuir–Blodgett films,[23–24] and assembling thick films by solvent evaporation.[31–33] However, most of these studies involved metal-nanoparticle assemblies.[35–36]

In this paper we describe the formation and characterization of PLA nanoparticles that are assembled on surface-modified 316L stainless steel through electrostatic interactions. The strategy involved a simple two-step process. The first step comprises the electrochemically induced formation of a positively charged self-assembled monolayer (SAM) in which the PLA nanoparticles were electrostatically attached to the SAM as a result of their negative charge. Recently we reported the electrochemically induced formation and characterization of *n*-alkanoic acid SAMs on 316L stainless steel surfaces.[15] We showed that the carboxyl group has a superior affinity for stainless steel and results in a highly organized monolayer that depends on the length of the alkyl chain. Following this line of research, we have successfully attached negatively charged PLA nanoparticles onto a positively charged 12-aminodecanoic acid (ADA) SAM. This approach offers a significant advantage because it allows the release of the drug, which contains PLA nanoparticles, to be controlled by changing the pH. We found that the surface density of the nanoparticles is controlled by the immersion time and the number of cyclic voltammetry (CV) scans under which the SAM was formed.

Results and Discussion

The electrostatically induced nanoparticle array was assembled by a simple two-step process. The first consists of the formation of a 12-aminododecanoic acid (ADA) SAM on a 316L stainless steel plate electrode (Scheme 1, step I). The second step involves the electrostatic attachment of PLA or gold nanoparticles onto a positively charged ADA SAM by immersing the stainless steel surface into the nanoparticle solution (Scheme 1, step II).

Formation and characterization of an ADA monolayer on 316L stainless steel: An ADA SAM was formed by means of our previously described method.[15] In essence, we showed that a highly organized SAM was formed by alternating the potential of 316L stainless steel in acetonitrile in the presence of sub-millimolar quantities of an alkanoic acid. It should be noted that small quantities of a 0.1 M aqueous solution of $HClO_4$ were required to dissolve the ADA. Figure 1 illustrates the effect of the number of potential scans, under which the monolayer is formed, on the CV of ferrocene (Fc). It is evident that the magnitude of the reduction and oxidation waves of Fc is reduced as the number of cycles increases. After ten cycles a "blocking effect" of Fc is observed (Table 1). The control experiment (Figure 1), in which a stainless steel disk electrode was swept for ten cycles in an acid-free CH_3CN solution, only affected the oxidation wave without affecting the electrochemical reversibility (for further details see ref. [9]). This result clearly indicates that blocking of the electrode is a result of the poten-

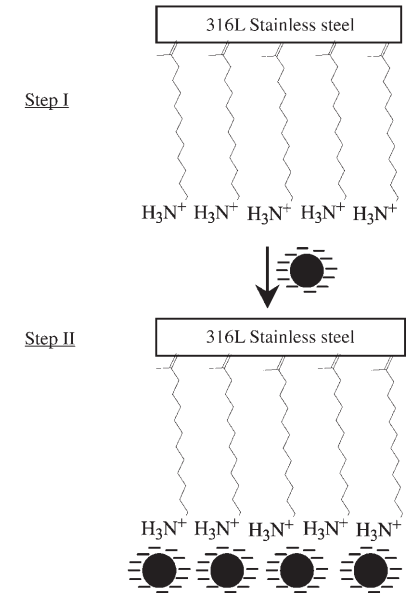

Scheme 1. Formation of a PLA or an Au nanoparticle film on a stainless steel plate.

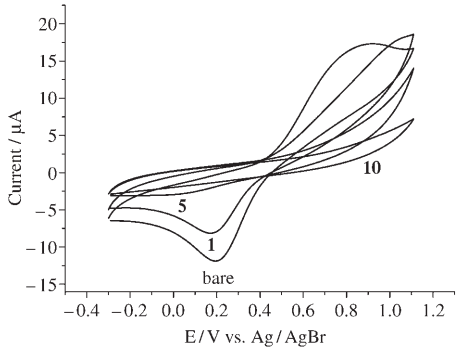

Figure 1. Cyclic voltammetry of a solution that contains ferrocene (1 mM) and TBATFB (0.1 M) in CH_3CN recorded with a bare 316L stainless steel electrode, and after electrochemical modification of the electrode in a solution that contains 12-aminododecanoic acid (0.1 mM) and TBATFB (0.1 M) in CH_3CN for 1, 5, and 10 cycles by applying a scan rate of 100 mV s^{-1}.

Table 1. Peak currents and potentials of the cathodic wave of Fc, as shown in Figure 1.

	Peak current [μA]	Reduction peak potential (V vs. Ag/AgBr)
bare electrode	12.0	0.193
1 CV scan	8.1	0.173
5 CV scans	≈3.0	≈−0.118
10 CV scans	no peak	no peak

tial-induced deposition of an alkanoic acid monolayer. The reduction peak potential was only 20 mV more negative and its current decreased by only 33% upon a single scan. The reduction peak current becomes negligible after five scans, whereas complete blocking is attained after ten cycles. This result suggests that ten CV scans between −0.8 and 1.2 V versus Ag/AgBr at a scan rate of 100 mV s^{-1} are sufficient to form a dense film.

The presence of an amino-terminated SAM was verified by X-ray photoelectron spectroscopy (XPS). Figure 2 shows the high-resolution XPS spectra of N_{1s} for an ADA-modified

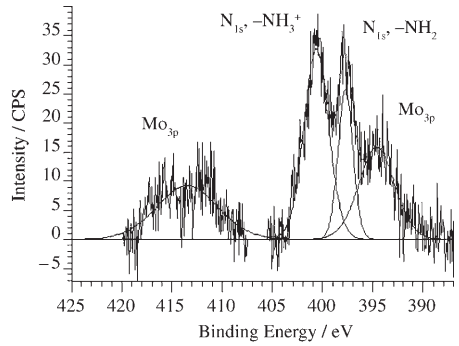

Figure 2. High-resolution N_{1s} XPS spectra of electrochemically treated stainless steel surface in the presence of ADA.

plate electrode after ten scans. The detection of nitrogen indicates successful film deposition because this element is only contained in the film material. It should be noted that amines were not detected on a bare stainless steel plate. The N_{1s} peak splits into two different nitrogen species at 397.9 and 401.1 eV, which are associated with aliphatic and protonated amino groups, respectively.[38–40] Deconvolution of these peaks gave a ratio of around 3:1 for $-NH_3^+$ and $-NH_2$, which implies that there are more protonated species than free aliphatic amino groups. It should, however, be remembered that the electrochemical deposition of the ADA SAM was carried out in the presence of $HClO_4$. The elemental ratio between carbon and nitrogen (derived from C_{1s} and N_{1s} high resolution spectra, respectively) was around seven, which is lower than the theoretical value, that is, larger than twelve (owing to the aliphatic carbon plus the carbon originating from the stainless steel). This result can be explained only if it is assumed that an organized monolayer has formed in which nitrogen is located on top of the layer and carbon is buried inside the film, and therefore, its intensity is reduced.

The formation of an ADA monolayer was also confirmed by water contact-angle measurements. The advancing (θ_a) and receding (θ_r) water contact angles of an ADA-modified stainless steel surface were $52\pm3°$ and $31\pm3°$, respectively, which are in good agreement with previous reports.[38,41,47] These surfaces show relatively large contact angle hystereses, which would be expected for polar and protic surface functionality.[48] Similar hysteresis values were published by Sukenik and Balachander[38] and Sieval and co-workers.[41] Sukenik and Balachander reported θ_a values of $62°\pm2°$ and $42°\pm3°$ and θ_r values of $42°\pm4°$ and $24°\pm4°$ for fully $-NH_2$- and $-NH_3^+$-terminated octadecyltrichlorosilane monolayers, respectively, and Sieval and co-workers reported contact angle values of $\theta_a = 63$–$68°$ and $\theta_r = 42°$. From the contact angle measurements and XPS data obtained we conclude that both protonated and unprotonated species are present in the ADA SAM.

External reflection absorbance Fourier transform infrared (RA-FTIR) spectroscopy was used to study the packing of the ADA SAM (Figure 3). The bands for the asymmetric

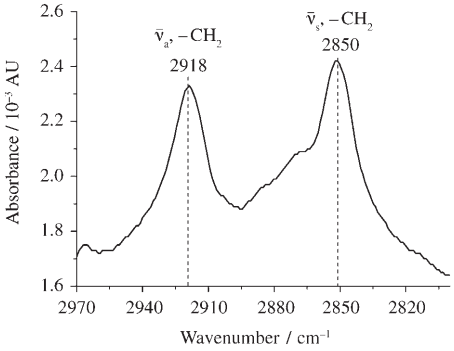

Figure 3. RA-FTIR spectrum of the asymmetric ($\tilde{\nu}_a$) and symmetric ($\tilde{\nu}_s$) C–H stretching region of a 316L stainless steel surface modified with ADA.

and symmetric methylene stretching modes appear at $\tilde{\nu} = 2918$ and 2850 cm^{-1}, respectively, and are indicative of a densely packed, highly ordered SAM. Direct detection of the amino groups in the ADA SAM is troublesome when using RA-FTIR spectroscopy owing to hydrogen bonding with adsorbed water molecules and −OH groups that originate from the stainless steel oxide. Nonetheless, after subtraction of the spectrum of the bare oxide surface from that of an ADA-modified surface, the NH_2 stretching mode could also be detected at $\tilde{\nu} = 3191$ cm^{-1} (not shown).

All of these findings indicate that an ADA monolayer forms a rather organized SAM on 316L stainless steel as a result of applying a sweeping potential to a solution in CH_3CN. This organized assembly is used, as described in the following section, as a means of electrostatically binding gold and PLA nanoparticles.

Immobilization of Au and PLA nanoparticles: Electrostatic assembly utilizes interactions between the negatively charged COO^- groups on the gold (citrate adsorbates) and PLA nanoparticle surfaces and the positively charged amine-functionalized monolayer. Figure 4 shows scanning electron microscopy (SEM) images of a bare stainless steel surface and an electrochemically induced ADA-SAM-modified stainless steel surface after immersion in Au and in PLA suspensions (pH 5 and pH 8) for 24 h. Evidently, a densely packed nanoparticle film is deposited on the modified surfaces at pH 5, whereas deposition of nanoparticles at the bare electrode is not observed. As binding between the nanoparticles and the modified surface is electrostatically driven, it is expected that the pH will play a major role in controlling the particle density on the surface. The nanoparticles, which are stabilized by carboxylic acid moieties, are negatively charged at $pH > \approx 4.5$. On the other hand, the amino-terminated monolayer is positively charged at pH values that are well below the pK of the aliphatic amines outside the monolayer. Knoll et al.[42,43] have shown that protonation of amino-terminated monolayers on Au commences below $pH \approx 6$. Therefore, for the pH values used, one can systematically vary the charge on the amine molecules while the carboxylic acid groups on the nanoparticles remain fully ionized, thereby altering the strength of the electrostatic interactions. At pH 4 to 5, the surface charge density on the amine-terminated monolayer is expected to attain its maximum charge, whereas at pH 8, the monolayer is completely unprotonated, which leads to a lower surface coverage. Furthermore, owing to the negative charge of the nanoparticles, a repulsive force between the particles in solution and those immobilized on the substrate prevents the nanoparticles from aggregating on the ADA SAM.

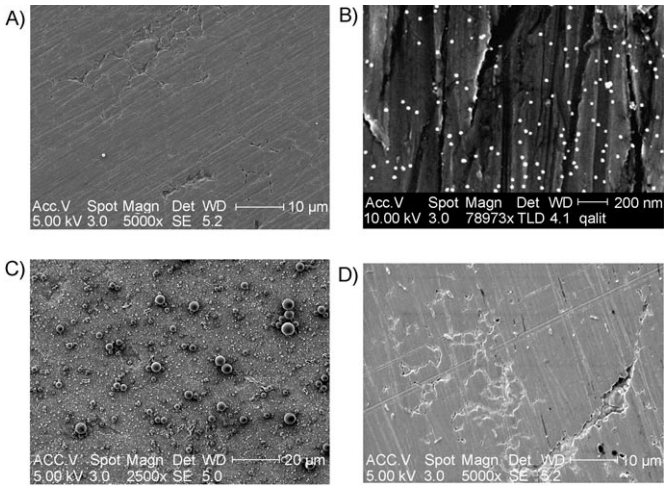

Figure 4. SEM images of a bare stainless steel surface (A) and an ADA-SAM-modified stainless steel surface immersed overnight in gold (16 nm) nanoparticles (B), and PLA (86% 2 µm and 14% 140 nm) nanoparticle suspensions at pH 5 (C) and pH 8 (D).

Additional support for electrostatic binding between the nanoparticles and the monolayer can be found from the fact that desorption of the nanoparticles occurs upon immersion of the steel in the solution at $pH > 8$, whereby the amine is deprotonated, and at $pH < 4$, whereby the carboxyl is protonated (Figure 5). Indeed, we found that gold nanoparticles desorbed at $8 < pH < 4$. On the other hand, the PLA nanoparticles desorbed at $pH > 8$, however, their surface coverage increased as pH decreased, even below pH 4. Moreover, our preliminary experiments show surprising morphological changes in the PLA nanoparticle (88 nm) films (Figure 6).[46] These changes will be discussed in a future manuscript.

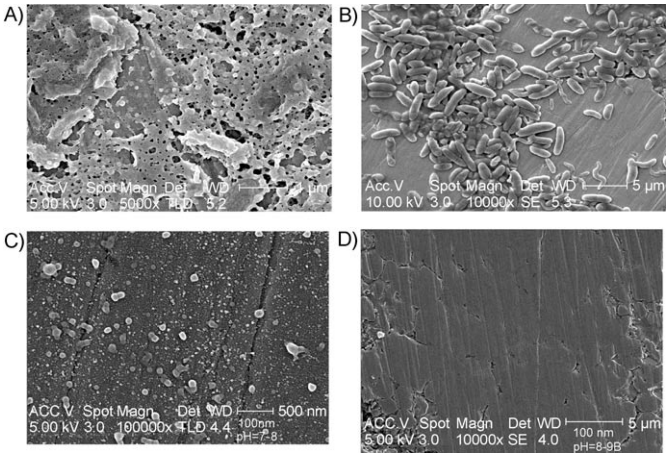

Figure 5. SEM images of 316L stainless steel surfaces that were modified in a solution of ADA (0.1 mM), TBATFB (0.1 M), and $HClO_4$ (0.1 M, 50 µL) in CH_3CN for 10 cycles, by applying a scan rate of 100 $mV\,s^{-1}$ and then immersing the surface overnight in a suspension of PLA nanoparticles (88 nm) at pH 4, 6, 7, and 8, respectively (A–D).

The effect of the number of potential scans under which the ADA SAM is formed on the surface density of the PLA nanoparticles is shown in Figure 7. It is clear that the PLA film density increases with the number of potential scans. No further improvement in the nanoparticle film density is observed when more than ten potential scan cycles are performed. This trend is in agreement with the cyclic voltammetry, which implies that the monolayer becomes denser with increasing the number of potential scans, presumably, by creating more interaction sites for the PLA binding.

The effect of immersion time on the surface density of the nanoparticles is shown in Figure 7. The stainless steel surfaces were exposed to ten cycles in a solution of tetrabutylammonium tetrafluoroborate (TBATFB, 0.1 M), $HClO_4$ (0.1 M, 50 µL), and ADA (0.1 mM) in CH_3CN. Subsequently, the electrodes were washed and immersed in a suspension of PLA nanoparticles (100 nm) at pH 5 for 1.5, 6, and 24 h. It is clear that as the immersion time increases, the density of the nanoparticles also increases. We did not observe a further increase in film density when immersing the modified electrodes for more than 24 h, which suggests that the layer had reached its final organization.

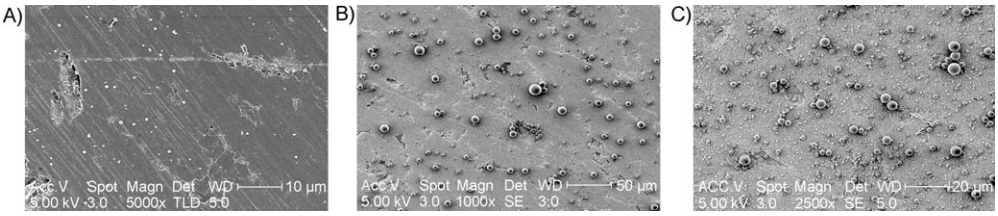

Figure 6. SEM images of 316L stainless steel surfaces that were modified in a solution of ADA (0.1 mM), TBATFB (0.1 M), and $HClO_4$ (0.1 M, 50 μL) in CH_3CN for 1 (A), 5 (B), and 10 (C) cycles by applying a scan rate of 100 $mV\,s^{-1}$ and then immersing the surface overnight in a suspension that contained PLA (86% 2 μm and 14% 140 nm) nanoparticles at pH 5.

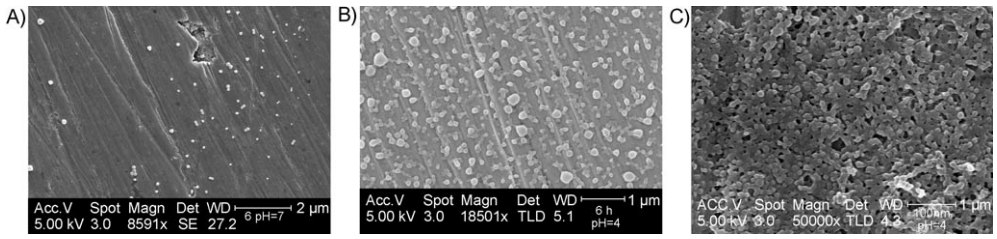

Figure 7. SEM images of an ADA-SAM-modified stainless steel surface immersed in a suspension of PLA nanoparticles in CH_3CN at pH 5, for 1.5 (A), 6 (B), and 24 h (C).

Conclusion

The electrostatically driven assembly of organic nanoparticles based on poly(lactic acid) and a positively charged monolayer on 316L stainless steel has been demonstrated. In a mildly alkaline solution (pH 8), in which the amino groups were not protonated, PLA nanoparticles could not be adsorbed onto the substrate, whereas under acidic conditions protonation makes the amino groups positively charged and adsorption of nanoparticles occurs. The density of the particles on the surface, which depends on the degree of interaction, could be controlled by varying the surface charge density of the monolayer (number of CV scans), immersion time, and by changing the pH of the nanoparticle solution. Finally, the approach presented here allows, in principle, the amount of drug accommodated in biodegradable nanoparticles to be controlled and to be attached onto an implantable medical device.

Experimental Section

Materials: ADA (95%), TBATFB (99%), and Fc (98%) were purchased from Aldrich. Acetonitrile (>99.8%) was obtained from J.T. Baker. Poly(DL-lactic acid) (M_W=112000) was synthesized in our laboratories. Dichloromethane and acetone (HPLC grade) were obtained from Biolab Jerusalem. Pluronic F-68 was obtained from Sigma. 316L Stainless steel plates and rods were obtained from Mashaf. The stainless steel plates (9×40 mm) were used for RA-FTIR, XPS, and contact angle measurements, whereas the rods were applied for electrochemical measurements (cyclic voltammetry). The stainless steel rod (3 mm diameter) was embedded in a Teflon sheath to expose only a disc, which served as the electrode surface.

Instrumentation: Electrochemical measurements were conducted with an AUTOLAB PGSTAT10 potentiostat (EcoChemie) and a BAS-100B/W electrochemical analyzer (Bioanalytical Systems), by using a single-compartment three-electrode glass cell. The reference electrode was an Ag/AgBr wire, which was prepared as previously described.[15] This reference electrode (0.45 V vs. ferrocene–ferrocenium[31]) is considerably more stable in the organic media than the commonly used Ag/AgCl wire. A graphite rod (6 mm diameter) was used as an auxiliary electrode.

RA-FTIR spectra were recorded by using a Bruker Equinox 55 spectrometer at a resolution of 2 cm^{-1}, which was equipped with a nitrogen-cooled mercury–cadmium–telluride detector. The spectra were acquired with a grazing-angle accessory that had an incident angle of 800 to the normal and a p-polarized beam. Normally, 1000 scans of the sample were collected versus a reference, which was a bare, freshly polished stainless steel surface.

XPS spectra were recorded by using a Kratos Axis Ultra spectrometer and $Mg_{K\alpha}$ radiation of 1486.71 eV. Data were collected and analyzed by using the vision processing program. Deconvolution of the peaks was conducted by using CasaXPS processing software (Casa Software, UK). Contact angles were measured with a Ramé-Hart model 100 contact angle goniometer. Advancing and receding contact angles were determined by adding and withdrawing fixed amounts of deionized water to and from the drop, respectively. This measurement was repeated three times for each sample and the average values are reported. All aqueous solutions were prepared from deionized water (Barnstead Easypure UV system).

A high-performance particle sizer (HPPS, ALV-GmBH) was used to determine the size and distribution of the nanoparticles.

Electrochemical procedures: The stainless steel disk electrodes were treated as previously described.[15] The plates were received, polished, and only treated with 1200 grit emery paper. The electrodes were then washed with CH_3CN and dried with a stream of nitrogen at room temperature prior to modification. The clean electrodes were immersed into a modification solution that contained ADA (0.1 mM), perchloric acid (50 μL, 0.1 M), and TBATFB (0.1 M) in CH_3CN at room temperature. A potential sweep between −0.8 to 1.2 V versus Ag/AgBr was typically applied (ten cycles unless otherwise stated). The modified surfaces were rinsed with pure CH_3CN and dried with a gentle stream of nitrogen. All measurements were performed at room temperature (21±2°C).

Formation and characterization of nanoparticles: Aqueous PLA nanoparticles that had an average particle size of ≈100±10 nm, ≈140±10 nm, and 2 μm±200 nm (confirmed by HPPS) were synthesized by employing a solvent extraction/evaporation method (single emulsion). A solution of

the polymer (100 mg) in dichloromethane (0.5 mL) and acetone (15 mL) was rapidly poured into an aqueous solution (40 mL) of Pluronic F-68 (80 mg) and stirred for a few minutes at room temperature. The solvents were evaporated under vacuum and the resulting oil-in-water emulsion was concentrated to about 10 mL. The size of the nanoparticles formed was determined by using ALV-NIBS/HPPS after dilution with water at 25 °C. The pH of the colloidal suspensions was about 5.

The gold nanoparticles (16 nm size, determined by nanosizer) were synthesized by following the method reported by Frens.[44] The zeta potential (−34.5 mV) measured by Zetasizer (Malvern Instruments) indicated that the nanoparticles were negatively charged in the solution (pH 5). The same solution was used for the gold nanoparticle assembly.

Specifically, PLA nanoparticles were assembled on an ADA-modified 316L stainless steel surface by immersing the modified substrate into an aqueous PLA suspension overnight. Then, the stainless steel was thoroughly rinsed with water and dried under ambient conditions.

Acknowledgements

This work was supported by the Hebrew University of Jerusalem through an applied grant and by Elutex. The unit for nanocharacterization of the Hebrew University of Jerusalem is acknowledged. This work was supported in part by a grant from the Israel Science Foundation (ISF).

[1] F. Zhang, E. T. Kang, P. Wang, K. L Tan, *Biomaterials* **2001**, *22*, 1541–1548.
[2] a) E. De Giglio, M. R. Guascito, L. Sabbatini, G. Zambonin, *Biomaterials*, **2001**, 22, 2609–2616; b) E. De Giglio, L. Sabbatini, P. G. Zambonin, *J. Biomater. Sci., Polym. Ed.* **1999**, *10*, 845–858; c) E. De Giglio, L. Sabbatini, S. Colucci, G. Zambonin, *J. Biomater. Sci., Polym. Ed.* **2000**, *11*, 1073–1083; d) E. De Giglio, L. De Gennaro, L. Sabbatini, G. Zambonin, *J. Biomater. Sci., Polym. Ed.* **2001**, *12*, 63–76.
[3] L. A. Guzman, V. Labhasertwar, C. Song, Y. Jang, A. M. Lincoff, R. Levy, E. J. Topol, *Circulation* **1996**, 94, 1441–1448.
[4] I. Fishbein, M. Chorny, L. Rabinovich, S. Banai, I. Gati, G. Golomb, *J. Controlled Release* **2000**, 65, 221–229.
[5] R. Gref, A. Domb, P. Quellac, T. Blunk, R. H. Muller, J. M. Verbavatz, R. Langer, *Adv. Drug Delivery Rev.* **1995**, *16*, 215–233.
[6] J. Panyam, D. Williams, A. Dash, D. Leslie-Pelecky, V. Labhasetwar, *J. Pharm. Sci.* **2004**, *93*, 1804–1814.
[7] J. M. Anderson, M. S. Shive, *Adv. Drug Delivery Rev.* **1997**, 28, 5–24.
[8] Z. Tang, Y. Wang, P. Podsiadlo, N. A. Kotov, *Adv. Mater.* **2006**, *18*, 3203–3224.
[9] G. Decher, J. D. Hong, J. Schmitt, *Thin Solid Films* **1992**, 210, 831–835.
[10] G. Decher, *Science* **1997**, *277*, 1232–1237.
[11] G. Decher, J. D. Hong, J. Schmitt, *Thin Solid Films* **1992**, 210, 831–835.
[12] N. Jessel, F. Atalar, P. Lavalle, J. Mutterer, G. Decher, P. Schaaf, J.-C. Voegel, J. Ogier, *Adv. Mater.* **2003**, *15*, 692–695.
[13] J. Chluba, J.-C. Voegel, G. Decher, P. Erbacher, P. Schaaf, J. Ogier, *Biomacromolecules* **2001**, *2*, 800–805.
[14] Z. Weiss, D. Mandler, G. Shustak, A. J. Domb, *J. Polym. Sci., Part A: Polym. Chem.* **2004**, *42*, 1658–1667.
[15] G. Shustak, A. J. Domb, D. Mandler, *Langmuir* **2004**, *20*, 7499–7506.
[16] G. Shustak, A. J. Domb, D. Mandler, *Langmuir* **2006**, *22*, 5237–5240.
[17] G. Shustak, M. Gadzinowski, S. Slomkowski, A. J. Domb, D. Mandler, *New J. Chem.* **2007**, *31*, 163–168.
[18] G. Chumanov, K. Sokolov, B. W. Gregory, T. M. Cotton, *J. Phys. Chem.* **1995**, *99*, 9466–9471.
[19] V. L. Colvin, A. N. Goldstein, A. P. Alivisatos, *J. Am. Chem. Soc.* **1992**, *114*, 5221–5230.
[20] A. Gole, S. R. Sainkar, M. Sastry, *Chem. Mater.* **2000**, *12*, 1234–1239.
[21] K. C. Grabar, P. C. Smith, M. D. Musick, J. A. Davis, D. G. Walter, M. A. Jackson, A. P. Guthrie, M. J. Natan, *J. Am. Chem. Soc.* **1996**, *118*, 1148–1153.
[22] K. Bandyopadhyay, V. Patil, K. Vijayamohanan, M. Sastry, *Langmuir* **1997**, *13*, 5244–5248.
[23] F. C. Meldrum, N. A. Kotov, J. H. Fendler, *J. Phys. Chem.* **1994**, *98*, 4506–4510.
[24] F. C. Meldrum, N. A. Kotov, J. H. Fendler, *J. Phys. Chem.* **1994**, *98*, 2735–2738.
[25] Z. L. Wang, S. A. Harfenist, R. L. Whetten, J. Bentley, N. D. Evans, *J. Phys. Chem. B* **1998**, *102*, 3068–3072.
[26] J. R. Heath, C. M. Knobler, D. V. Leff, *J. Phys. Chem. B* **1997**, *101*, 189–197.
[27] S. Connolly, S. Fullam, B. Korgel, D. Fitzmaurice, *J. Am. Chem. Soc.* **1998**, *120*, 2969–2970.
[28] Y. Taguchi, R. Kimura, R. Azumi, H. Tachibana, N. Koshizaki, M. Shimomura, N. Momozawa, H. Sakai, M. Abe, M. Matsumoto, *Langmuir* **1998**, *14*, 6550–6555.
[29] Y. Lvov, K. Ariga, I. Ichinose, T. Kunitake, *J. Am. Chem. Soc.* **1995**, *117*, 6117–6123.
[30] K. C. Grabar, P. C. Smith, M. D. Musick, J. A. Davis, D. G. Walter, M. A. Jackson, A. P. Guthrie, M. J. Natan, *J. Am. Chem. Soc.* **1996**, *118*, 1148–1153.
[31] M. D. Musick, C. D. Keating, L. A. Lyon, S. L. Botsko, D. J. Pena, W. D. Holliway, T. M. McEvoy, J. N. Richardson, M. J. Natan, *Chem. Mater.* **2000**, *12*, 2869–2881.
[32] A. N. Shipway, M. Lahav, R. Gabai, I. Willner, *Langmuir* **2000**, *16*, 8789–8795.
[33] A. N. Shipway, M. Lahav, I. Willner, *Adv. Mater.* **2000**, *12*, 993–998.
[34] G. Ladam, P. Schaaf, G. Decher, J. C. Voegel, F. J. G. Cuisinier, *Biomol. Eng.* **2002**, 19, 273–280.
[35] S. Liu, R. Hu, Z. Liu, *Phys. Chem. Chem. Phys.* **2002**, *4*, 6059–6062.
[36] T. Zhu, X. Fu, J. Wang, Z. Liu, *Langmuir* **1999**, *15*, 5197–5199.
[37] G. Gritzner, G. Kuta, *Pure. Appl. Chem.* **1984**, 56, 461–466.
[38] N. Balachander, C. N. Sukenik, *Langmuir* **1990**, *6*, 1621–1627.
[39] K. Bierbaum, M. Kinzler, Ch. Woell, M. Grunze, G. Haehner, S. Heid, F. Effenberger, *Langmuir* **1995**, *11*, 512–518.
[40] A. E. Hooper, D. Werho, T. Hopson, O. Palmer, *Surf. Interface Anal.* **2001**, 31, 809–814.
[41] A. B. Sieval, R. Linke, G. Heij, G. Meijer, H. Zuilhof, E. J. R. Sudholter, *Langmuir* **2001**, *17*, 7554–7559.
[42] R. Schweiss, P. B. Welzer, C. Werner, W. Knoll, *Langmuir* **2001**, *17*, 4304–4311.
[43] R. Schweiss, C. Werner, W. Knoll, *J. Electroanal. Chem.* **2003**, 540, 145–151.
[44] G. Frens, *Nature Phys. Sci.* **1973**, 241, 20–22.
[45] T. Zhu, F. X. Fu, T. Mo, J. Wang, Z. F. Liu, *Langmuir* **1999**, *15*, 5197–5199.
[46] G. Shustak, A. J. Domb, D. Mandler, unpublished results.
[47] A. Heise, M. Stamm, M. Rauscher, M. Duscher, H. Menzel, *Thin Solid Films* **1998**, 199–203.
[48] C. D. Bain, E. B. Troughton, Y.-T. Tao, J. Evall, G. Whitesides, R. G. Nuzzo, *J. Am. Chem. Soc.* **1989**, *111*, 321–335.

Received: October 31, 2006
Published online: May 16, 2007

